REPORT DOCUMENTATION PAGE

1

Form Approved OMB NO. 0704-0188

1. REPORT DATE (DD-MM-YYYY)	2. REPORT TYPE	3. DATES COVERED (From - To)
17-09-2014	Final Report	25-Sep-2009 - 24-Apr-2014

4. TITLE AND SUBTITLE
Active Signal Propagation and Imaging Using Vortex Beams

5a. CONTRACT NUMBER
W911NF-09-1-0552

5b. GRANT NUMBER

5c. PROGRAM ELEMENT NUMBER
611102

6. AUTHORS
Robert Alfano

5d. PROJECT NUMBER

5e. TASK NUMBER

5f. WORK UNIT NUMBER

7. PERFORMING ORGANIZATION NAMES AND ADDRESSES
CUNY - City College of New York
Research Foundation of CUNY
230 W 41st Street FL 7
New York, NY 10036 -7207

8. PERFORMING ORGANIZATION REPORT NUMBER

9. SPONSORING/MONITORING AGENCY NAME(S) AND ADDRESS (ES)
U.S. Army Research Office
P.O. Box 12211
Research Triangle Park, NC 27709-2211

10. SPONSOR/MONITOR'S ACRONYM(S)
ARO

11. SPONSOR/MONITOR'S REPORT NUMBER(S)
52759-PH-H.15

12. DISTRIBUTION AVAILIBILITY STATEMENT
Approved for Public Release; Distribution Unlimited

13. SUPPLEMENTARY NOTES
The views, opinions and/or findings contained in this report are those of the author(s) and should not contrued as an official Department of the Army position, policy or decision, unless so designated by other documentation.

14. ABSTRACT
The objective of this research project was to circumvent scattering obstacles for optical signal propagation and imaging through turbid media, making use of the phase singularity and orbital angular momentum of vortex beams. The specific aims of the project were:
(1) Develop a guide-probe technique that guides the signal beam into turbid media with optical vortex beams, carrying orbital angular momentum. Unlike more conventional methods that have to bear the deteriorated scattered light, this innovative technique was based on the ability of an optical vortex guide beam to bear a transient viewing

15. SUBJECT TERMS
imaging, complex light, vortex beams

16. SECURITY CLASSIFICATION OF:			17. LIMITATION OF ABSTRACT	15. NUMBER OF PAGES	19a. NAME OF RESPONSIBLE PERSON
a. REPORT	b. ABSTRACT	c. THIS PAGE			Robert Alfano
UU	UU	UU	UU		19b. TELEPHONE NUMBER 212-650-5531

Report Title

Active Signal Propagation and Imaging Using Vortex Beams

ABSTRACT

The objective of this research project was to circumvent scattering obstacles for optical signal propagation and imaging through turbid media, making use of the phase singularity and orbital angular momentum of vortex beams. The specific aims of the project were:
(1) Develop a guide-probe technique that guides the signal beam into turbid media with optical vortex beams, carrying orbital angular momentum. Unlike more conventional methods that have to bear the deteriorated scattered light, this innovative technique was based on the ability of an optical vortex guide beam to bore a transient viewing path in the medium. Imaging through this path experienced less obstacle scattering events and in turn enhanced contrast and resolution of the image.
(2) Investigate the degradation of the orbital angular momentum by turbid media and the optical memory effect and evaluate its capability for providing discrimination against multiply scattered light and thus facilitating imaging through turbid media.
(3) Investigate the ability to generate a tunable optical filter using optical vortex light in concert with supercontinuum and a novel liquid crystal q-plate.
Significant progress was achieved accomplishing these aims.
The outcome of research has interested Corning in supporting and enhancing the research.

Enter List of papers submitted or published that acknowledge ARO support from the start of the project to the date of this printing. List the papers, including journal references, in the following categories:

(a) Papers published in peer-reviewed journals (N/A for none)

Received		Paper
05/07/2012	8.00	Giovanni Milione, H. I. Sztul, D. A. Nolan, R. R. Alfano. Higher-Order Poincaré Sphere, Stokes Parameters, and the Angular Momentum of Light, Physical Review Letters, (07 2011): 53601. doi: 10.1103/PhysRevLett.107.053601
09/17/2014	14.00	Giovanni Milione, Robert R Alfano, Pavel Shumyatsky. Optical memory effect from polarized Laguerre–Gaussian light beam in light-scattering turbid media, Optics Communications, (06 2014): 0. doi: 10.1016/j.optcom.2014.01.039
11/28/2012	9.00	Giovanni Milione, S. Evans, D. Nolan, R. Alfano. Higher Order Pancharatnam-Berry Phase and the Angular Momentum of Light, Physical Review Letters, (05 2012): 0. doi: 10.1103/PhysRevLett.108.190401
TOTAL:		**3**

Number of Papers published in peer-reviewed journals:

(b) Papers published in non-peer-reviewed journals (N/A for none)

Received		Paper
TOTAL:		

Number of Papers published in non peer-reviewed journals: 3

(c) Presentations

Number of Presentations: 3.00

Non Peer-Reviewed Conference Proceeding publications (other than abstracts):

Received	Paper	
05/07/2012	2.00	Giovanni Milione, Stefan Evans, Robert R. Alfano. Hybrid vector beam generation, Complex Light and Optical Forces V. 26-JAN-11, San Francisco, California, USA. : ,
05/07/2012	3.00	Giovanni Milione, H. I. Sztul, Robert R. Alfano. Geometric phase associated with transformations of cylindrical vector beams, Complex Light and Optical Forces V. 26-JAN-11, San Francisco, California, USA. : ,
05/07/2012	4.00	Giovanni Milione, Jeff Secor, Greg Michel, Stefan Evans, Robert R. Alfano. Raman optical activity by light with spin and orbital angular momentum, Complex Light and Optical Forces V. 26-JAN-11, San Francisco, California, USA. : ,
05/07/2012	5.00	G. Milione, H. I. Sztul, D. A. Nolan, J. Kim, M. Etienne, J. McCarthy, J. Wang, R. R. Alfano. Cylindrical vector beam generation from a multi elliptical core optical fiber, Complex Light and Optical Forces V. 26-JAN-11, San Francisco, California, USA. : ,
11/28/2012	10.00	Giovanni Milione, Stefan Evans, Daniel Nolan, Robert Alfano. The Geometric Phase and Singular Light Beams, Conference on Lasers and Electro-Optics (CLEO), paper JTh3K.6 . 07-MAY-12, . : ,
TOTAL:	**5**	

Number of Non Peer-Reviewed Conference Proceeding publications (other than abstracts): 4

Peer-Reviewed Conference Proceeding publications (other than abstracts):

Received	Paper	
08/27/2013	13.00	S Evans, D A Nolan, R R Alfano, Giovanni Milione. The geometric phase and singular light beams, Lasers and Electro-Optics (CLEO), 2012 Conference on. 01-AUG-12, . : ,
11/28/2012	11.00	Giovanni Milione, Robert R. Alfano. A higher order Poincare sphere representation, SPIE OPTO. 06-FEB-12, San Francisco, California. : ,
11/28/2012	12.00	Giovanni Milione, Robert Alfano. Vector Beam Representation on a Higher Order Poincare Sphere and Higher Order Stokes Parameter Measurement Through Optical Angular Momentum Decomposition, Frontiers in Optics (FiO) OSA. 16-OCT-11, . : ,
TOTAL:	**3**	

Number of Peer-Reviewed Conference Proceeding publications (other than abstracts):

(d) Manuscripts

Received	Paper
TOTAL:	

Number of Manuscripts:

Books

Received	Book
TOTAL:	

Received	Book Chapter

TOTAL:

Patents Submitted

Patents Awarded

Awards

1. National Science Foundation Graduate Research Fellowship, Giovanni Milione 2011
2. SPIE International Society of Optics and Photonics Scholarship, Giovanni Milione 2011
3. Finalist, Emil Wolf Outstanding Student Paper Competition, Giovanni Milione (2011)
4. Robert R. Alfano, American Physical Society, Arthur L. Schawlow Prize in Laser Science (October, 2013)
5. Robert R. Alfano, City College of New York, President's Award For Excellence (2013)
6. Robert R. Alfano, Association of Italian-American Educators, Lifetime Achievement Award (2012).
7. Giovanni Milione, Optical Society of America, Finalist Emil Wolf Outstanding Student Paper Competition.

Graduate Students

NAME	PERCENT_SUPPORTED	Discipline
Giovanni, Milione	0.50	
Thien An Nguyen	1.00	
Lingyang Shi	0.50	
FTE Equivalent:	**2.00**	
Total Number:	**3**	

Names of Post Doctorates

NAME	PERCENT_SUPPORTED
FTE Equivalent:	
Total Number:	

Names of Faculty Supported

NAME	PERCENT_SUPPORTED	National Academy Member
Robert Alfano	0.10	
FTE Equivalent:	**0.10**	
Total Number:	**1**	

Names of Under Graduate students supported

NAME	PERCENT_SUPPORTED	Discipline
Zabir Hossain	1.00	Physics
Laura Sordillo	1.00	Physics
Grech Sabina	0.50	
Samuel Nuzbrokh	0.20	Physics
Richard Gozali	0.50	Physics
Leana Wang	0.20	
Jonna Turesson	0.20	Physics
Caterine Taballione	0.30	
Rory McGriskin	0.30	
Hussain Bokhari	0.20	
Maxwell Anderson	0.20	
FTE Equivalent:	**4.60**	
Total Number:	**11**	

Student Metrics

This section only applies to graduating undergraduates supported by this agreement in this reporting period

The number of undergraduates funded by this agreement who graduated during this period: 3.00

The number of undergraduates funded by this agreement who graduated during this period with a degree in science, mathematics, engineering, or technology fields:..... 3.00

The number of undergraduates funded by your agreement who graduated during this period and will continue to pursue a graduate or Ph.D. degree in science, mathematics, engineering, or technology fields:..... 3.00

Number of graduating undergraduates who achieved a 3.5 GPA to 4.0 (4.0 max scale):..... 1.00

Number of graduating undergraduates funded by a DoD funded Center of Excellence grant for Education, Research and Engineering:..... 0.00

The number of undergraduates funded by your agreement who graduated during this period and intend to work for the Department of Defense 0.00

The number of undergraduates funded by your agreement who graduated during this period and will receive scholarships or fellowships for further studies in science, mathematics, engineering or technology fields: 0.00

Names of Personnel receiving masters degrees

NAME
Total Number:

Names of personnel receiving PHDs

NAME
Total Number:

Names of other[7] research staff

NAME	PERCENT_SUPPORTED
Pavel Shumyatsky	0.50
Yury Budansky	0.30
Joan Brijlall	0.30
FTE Equivalent:	**1.10**
Total Number:	**3**

Sub Contractors (DD882)

Inventions (DD882)

Scientific Progress

See Attachment

Technology Transfer

Active Signal Propagation and Imaging Using Vortex Beams

Final Report 2014

August 1, 2014

Current Grant Number: W911NF-09-1-0552
Current Proposal Number: 52759-PH-H
Current Grant Officer Representative: Richard T. Hammond
Principal investigator: Robert R. Alfano

Abstract

This report gives overview of progress achieved on active signal propagation and imaging using vortex beams for grant W911NF-09-1-0552. The objective of this research project was to circumvent scattering obstacles for optical signal propagation and imaging through turbid media, making use of the phase singularity and orbital angular momentum of vortex beams. The specific aims of the project were:

(1) Develop a **guide-probe** technique that guides the signal beam into turbid media with optical vortex beams, i.e., Laguerre-Gaussian (LG) beams, carrying orbital angular momentum. Unlike more conventional methods that have to bear the deteriorated scattered light, this innovative technique was based on the ability of an optical vortex guide beam to bore a transient viewing path in the medium, analogous to the way that a hurricane can move an object. Imaging through this path experienced less obstacle scattering events and in turn enhanced contrast and resolution of the image.

(2) Investigate the degradation of the orbital angular momentum by turbid media and the optical memory effect and evaluate its capability for providing discrimination against multiply scattered light and thus facilitating imaging through turbid media.

(3) Investigate the ability to generate a tunable optical filter using optical vortex light in concert with supercontinuum and a novel liquid crystal q-plate.

Significant progress in basic understanding of complex light was achieved by the sixteen (17) papers, twenty two (22) presentations, and 7 awards. The outcome of research has interested Corning in supporting and enhancing the research.

Introduction

The report is divided into 4 topics: guide-probe technique, orbital angular momentum degradation and optical memory effect in scattering media, OAM dependence on polarization resolved image contrast improvement, and tunable optical vortex.

1. Guide-probe technique

The guide probe technique was based on a radial gradient force exerted on small particles by an optical vortex beam. We proposed an innovative active ballistic signal propagation and imaging approach that will use an optical vortex beam to bore a “short-lived” viewing path through a scattering medium to guide time-delayed information-carrying light. The radial gradient force is associated with the “donut-like” intensity of an optical vortex beam whose

electric field amplitude is given by:

$$u_{p,l}(r,f,z)=\frac{C_{p,l}}{w(z)}\left(\frac{r\sqrt{2}}{w(z)}\right)^{|l|}\exp\left(-\frac{r^2}{w(z)}\right)L_p^{|l|}\left(\frac{2r^2}{w^2(z)}\right)\exp\left(-\frac{ikr^2z}{2(z+z_R)}\right)$$

$$\times\exp(-ilf)\exp\left(i(2p+l+1)\arctan\left(\frac{z}{z_R}\right)\right)\quad(1)$$

where $C_{p,l}$ is the normalization constant, $L_p^{|l|}$ is the generalized Laguerre polynomial, p is the radial mode (any positive integer) and l is the azimuthal mode (any integer). The radius of the beam at position z is $w(z)=w(0)\sqrt{\left(z_R^2+z^2\right)/z_R^2}$. $w(0)$ is the width at the beam waist, and $\left(2p+l+1\right)\arctan(z/z_R)$ is the Gouy phase where z_R is the Rayleigh range. The order of the Laguerre-Gaussian mode is given by $N=2p+|l|$. The radial gradient force for small particles with a beam of $l = 1$ and $p = 0$ can be derived from Eq. (1):

$$F\propto\nabla I=\nabla_r\left(\frac{C^2}{w^2}\frac{2r^2}{w^2}\exp\left(-\frac{2r^2}{w^2}\right)\right)=\frac{4rC^2}{w^4}\left(1-\frac{2r^2}{w^2}\right)\exp\left(-\frac{2r^2}{w^2}\right)\quad(2)$$

The gradient force points to the intensity maxima of the Laguerre-Gaussian beam at $r_{\max}=w/\sqrt{2}$. It was demonstrated that optical vortex beams can trap high-index and low-index particles at the dark center when the particle size is close to the diameter of the dark area. The orbital angular momentum of photons can be transferred to microscopic particles and cause them to rotate around the circumference of the optical vortex .

1.1. Guide-probe experiment

Implementation of OV-GP imaging is based on the ability of an OV beam to move scattering particles away from beam axis via an outward “intensity gradient force” as described above. The force exerted on the scattering particles is directly proportional to the magnitude of the OV beam’s intensity; a high power (intensity) OV beam produces a large force. In previous years we generated an OV beam via the diffraction of a Gaussian beam from a reflective phase only spatial light modulator. Though this method of OV beam generation allows dynamic control it also results in poor power conversion efficiency (~< 15%) and relatively low power tolerance (~2W/cm2). Therefore, to achieve the high power required for OV-GP imaging, we use a new device called a liquid crystal radial polarizer (RP) (ARCoptix). The RP generates an OV beam via the transmission of a Gaussian beam resulting in higher conversion efficiency (~>85%) and higher power tolerance (~500W/cm2). As shown in Fig. 1 a horizontally polarized continuous wave Gaussian beam (Coherent: Verdi-V18, 532 nm, 0-20 W) is expanded and collimated to a diameter of ~10mm then propagates normally through the RP. The RP is a window of twisted liquid crystal molecules with azimuthally varying twist and operates like a half wave plate with azimuthally varying fast axis. Transformation of the state of polarization of the horizontally polarized Gaussian beam upon propagation through the RP can be described by a Jones matrix analysis:

$$\begin{pmatrix} \cos\theta & \sin\theta \\ \sin\theta & -\cos\theta \end{pmatrix} \begin{pmatrix} 1 \\ 0 \end{pmatrix} = \begin{pmatrix} \cos\theta \\ \sin\theta \end{pmatrix}$$

where θ is the azimuthal angle about the beam axis. As can be seen the horizontally polarized Gaussian beam becomes radially polarized. In contrast to the spatial light modulator that generates an OV possessing a **phase** singularity of the electromagnetic field the RP generates an OV possessing a **polarization** singularity. Nonetheless, upon diffraction into the far field the resulting OV beam develops the characteristic donut-like intensity distribution.

A Gaussian probe beam (633nm, 5mW, cw) was generated directly from a He-Ne laser. The wavelengths of the guide and probe beams are made different so they do not interfere and so they can be effectively combined using a dichroic beam splitter. As shown in Fig. 1(b) the guide and probe beams are combined, made to be strongly co-linear, and then focused to a diameter of 100 microns through a rectangular quart cell (1cm x 10 cm x 10cm). Various TM conditions are simulated inside the cell by diluting deionized water with polystyrene spheres of varying size and concentration. In this way, we can study OV-GP imaging as a function of OV beam power, scatterer size, and scatterer concentration. A second lens collects and collimates forward scattered light. Two marrow pass band filters (623.8 nm) are used to filter out the green OV beam from the transmitted Gaussian beam. A diffraction grating (1200 mm-1) is then used to further separate the red probe beam from any remaining green light. The transmitted intensity of the probe beam is then collected with a photodiode attached to a digital oscilloscope. We find the guide beam is effectively filtered from the probe beam; any residual green light is well below the photodiode noise level even when the guide beam is at maximum power as shown in Fig 1(b). To demonstrate the effectiveness of the guide-probe beam setup, the two beams were slightly misaligned, as shown in Fig. 1(c). Both beams were then focused into a 1cm x 1cm x 10cm glass cell comprising a solution of latex spheres and ionized water. Different particle sizes, d, corresponding to Rayleigh ($\lambda<d$) and Mie ($\lambda>d$) scattering were investigated for various solution concentrations and guide beam powers. The latex spheres will continuously diffuse in and out of the path of the probe beam between measurements due to Brownian motion. To account for this the intensity of the probe beam is measured over a 30 second time interval. The guide beam is turned at 10 seconds and then turned off at 20 seconds as shown in Fig. 1(b) and Fig. 1(c). Using this experimental setup, for a constant particle concentration and size, the transmitted intensity of the probe beam is measured as a function of the guide beam power and is plotted in Fig. 1(b) and 1(c). As can be seen the transmitted intensity of the probe beam increases linearly as a function of the guide beam power showing ~2% percent increase for 5W. The transmission of the probe beam as a function of particle size is shown in Fig. 3. As can be seen, for 3μm particles and a concentration of 0.75 x $10^{-}4$, the transmission of the probe beam increases as the guide beam power is increased.

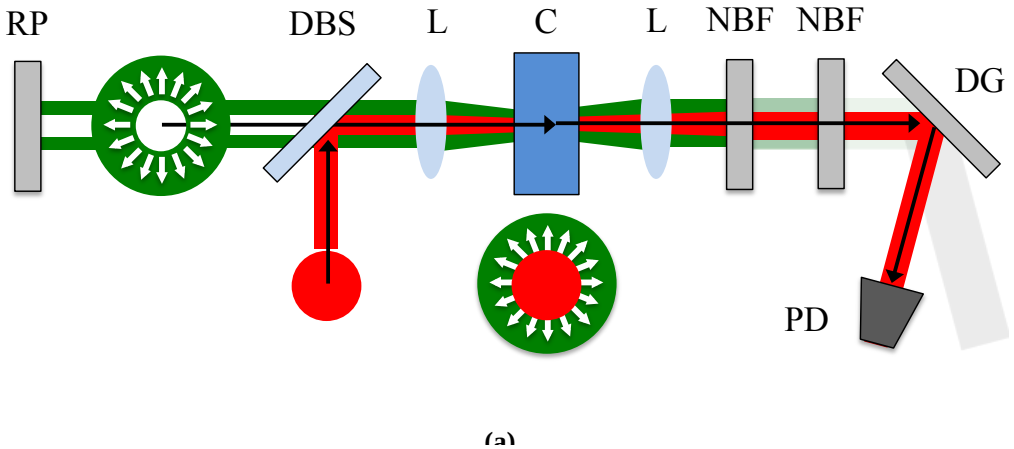

(a)

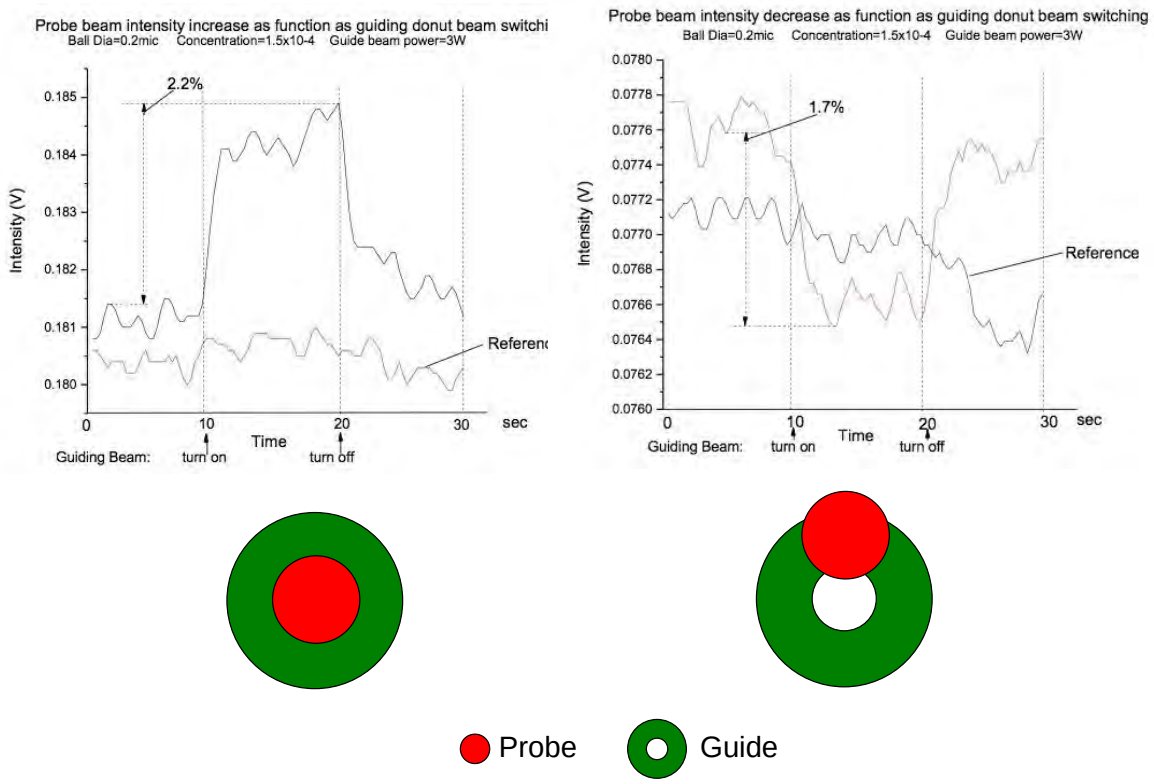

(b)

Figure 1. (a) A radial polarizer (RP) is used to generate an OV beam. A dichroic beam splitter (DBS)is used to combine the green OV guide beam and a red Gaussian probe beam. A lens (L) focuses the collinear beams into a cell (C) containing TM. A second lens (L) collimates and collects the two beams after the cell. Two narrow band filters (NBF) filter out the green guide beam. A diffraction gating (DG) is used to further separate the guide and probe beams. The separated probe beam is collected with a photo diode (PD). **(b)** Probe beam intensity dependence on guiding donut beam.

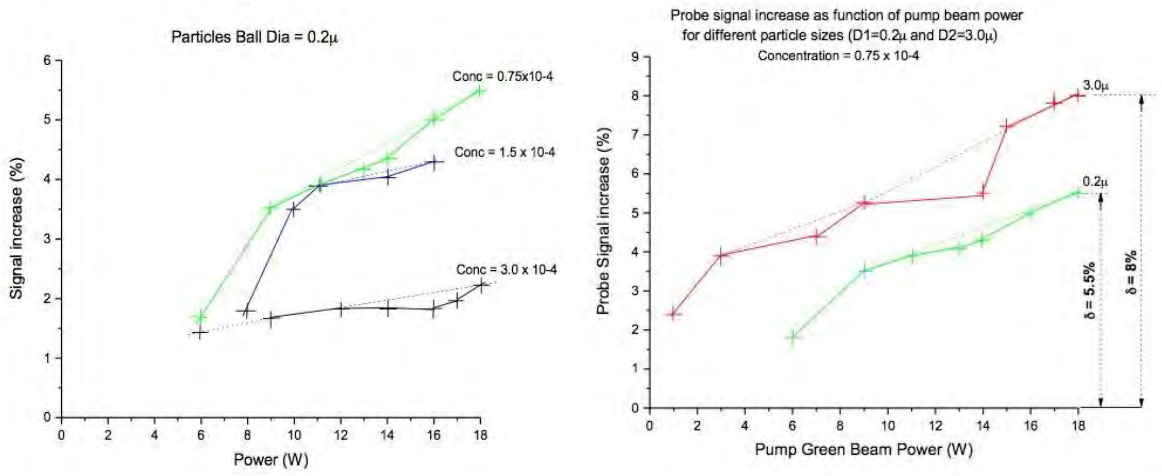

Figure 2. Transmission of the guide probe beam through the scattering media as a function of beam position and time delay (a) collinear guide probe (b) misaligned guide probe. Transmission as a function of particle size and concentration (c) .2 microns (d) 3 microns

1.2. Image Visibility Improvement

We investigated experimentally image visibility improvement using the guide-probe technique inside OV beam described above. A USAF glass target was located behind the cell with turbid media and imaged using the red probe beam. The images are shown in Fig. 3(a) and Fig. 3(b) for the guide beam turned off and on, respectively. The contrast profiles of these images as well as other images at different power of guiding donut light beam are shown in Fig. 3(c). It was determined that the image contrast of the target located in turbid media may be increased up to 12% using 18W guiding donut light beam.

(a) (b)

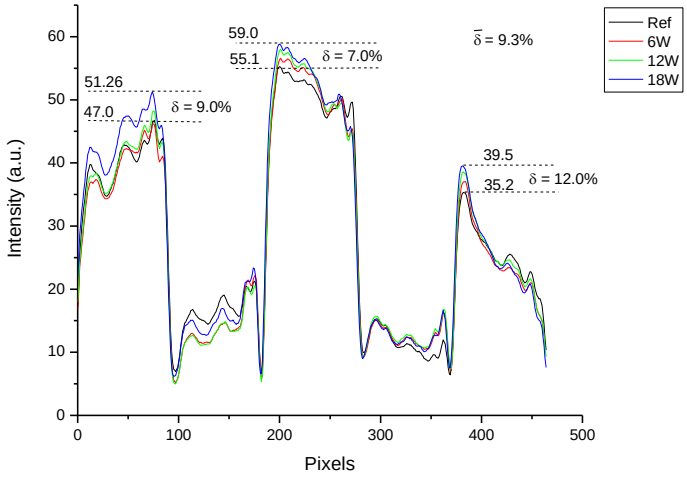

(c)

Fig. 3. Images and intensity profile of the target (USAF Glass) located behind turbid media. (a) Guiding donut light beam power is off. (b) 18 W guiding donut light beam is on. (c) Intensity profiles of the target at different guiding donut light beam powers.

2. Orbital angular momentum degradation and optical memory effect in scattering media

Polarized complex Laguerre-Gaussian light with different orbital angular momentum propagation in turbid media was investigated during this period. The Optical Memory Effect in scattering media with small and large size (compared with the wavelength) scatterers is investigated for polarized light using polarized laser modes with varying orbital strength L-parameter. It is shown, that backscatter image quality (contrast) can be enhanced by more than an order of magnitude by using the circularly polarized light.

The propagation and scattering of light in an optical dense turbid medium plays a significant role in communication, remote sensing and imaging of an object hidden in the scattering media. Scattering media blurs coded information and images. Using the salient properties of light: wavelength, coherence, and polarization one can improve image and coded information traveling in free space inside fog, clouds, smoke, and tissue as well as in optical fibers. Over the years, several methods have been used to discriminate the signal and improve the quality of an object image from the noise of scattered light. The problem to extract an image propagating through or located in a scatter medium was investigated theoretically and experimentally over past 20 years. One key and simple approach to improve image quality and information flow is to use the vector nature of light, which can play a key role in the process of the light scattering. Using a polarized laser beams, it was shown that the intensity of forward and backscattered light significantly depends on the size of the scattering particles, their concentration in a turbid medium and on the polarized state of the incident light beam. The three key length parameters important to characterize light propagating in scattering media are: the scattering length (Ls), transport lengths (Ltr) and absorption length (La). The Ls is the mean

distance between scatters; Ltr is the distance traveled to change the directions of incoming photons, and La is the distance where the photons are absorbed. These lengths are inverse of the scattering coefficients: μ_s, μ_{tr} and μ_a respectively. The scattering from small scatter particles are more random in direction after a scattering event, while from large scatter particles are more forwarded scatter. The sizes of scattering particles (d) are compared to wavelength of light: small size scatterers ($d<\lambda$) and large size particles ($d>\lambda$). The polarization techniques have been advanced to improve the imaging of a hidden object inside a highly optical dense turbid medium. It was shown experimentally that an image contrast of an object can be enhanced by linear polarized light because the parallel component of polarization vector is highly reflected off front surface and overwhelms any imaging information below the surface in backward scattering imaging. The perpendicular component blurs an image and travels deeper to give information below the surface. An alternative method using circularly polarized light gives possibility to significantly improve an imaging in a higher concentration (multi-scattering events) of a medium and mainly in the case of large size scatterers ($d>\lambda$, Mie scattering). In this case of scattering from high concentration of the large size particles, the backscattered light was shown to predominantly retain the same state of polarization at the incident light for both of polarizations (linear and circular). This phenomena is known as the ***Optical Memory Effect (OME***). A Twist of light is associated with the non-planar wave front of Laguerre–Gaussian which uses the property of orbital, L and spin angular momentum, S parameters. The strength L is associated with vortex of the wavefront twist and S is associated with the circular vector polarization.

The scattering and imaging is investigated in this program with different orbital angular momentum (OAM) states (L) for scattering media with small and large scattering particles. The parameter L is a measure of OAM and strength of the optical vortex of the LG-beams. The LG complex laser beams adds a new dimension of light's spatial degree of freedom to light propagating in turbid medium, includes helical shaped and twisted wave front, singularities of electric fields and spatial vector polarization states of the beam profile. These twisted special light forms opens a new renaissance era in optics called "complex vector light". This complex vector light can possess both spin angular momentum (SAM) which is associated with optical circular polarization and orbital angular momentum (OAM), which is associated with helicity of non-planar wave front. The angular momentum of spin and orbital properties appear separately and are not interacting in paraxial beams. Coupling can occur by the spin-orbit interaction (SOI) of SAM and OAM in non paraxial beams, highly focusing, scattering in inhomogeneous and anisotropic media.

The LG laser beam has an optical vortex (phase singularity) at the center of the beam and carries an orbital angular momentum (OAM: $\pm L\hbar$) and a spin angular momentum (SAM: $\sigma = \pm$), so the total angular moment is proportional to ($L+\sigma$).

The phase singularity (optical vortex) at the center of the beam is the point (area) of zero intensity and such beam has spatial profile of a ring and been called a "donut" beam.

In this research, two experimental geometrical arrangements were investigated: the angle (90˚) scattering and backscattering (180˚) for different orbital angular momentum modes L and state of polarization of the vortex LG beams. The polarized LG (donut) beams are used for investigation of scattering and imaging in the turbid medium with the scattering particles of the different sizes and concentrations (volume fraction of scatterers) in water solution. Small size scatterers ($d<\lambda$, the case of Rayleigh scattering) and the large size particles ($d>\lambda$) at the different concentration were studied for understanding of possible influence of the OAM L-effects on the OME-phenomena.

2.1. OAM Dependence on Scattered Light Depolarization

Light propagation in TM results in light scattering in well-defined directions depending on scattering particle size. The particle size and concentration is critical and greatly affects the SOP of the scattered light, being different than the SOP of the incident light beam (depolarization). Scattering increases for higher particle concentration and is different when the scattering particle size is larger or smaller than the wavelength of the scattered light. Experimental measurement of light's depolarization in TM therefore serves as a probe with which to characterize TM by the size and concentration of the scattering particles. Conversely, a light beam's depolarization in TM quantifies the amount it scatters. Interrogating a TM with an OV light beam may effect the light's depolarization and serves as a direct indication of the ability of an OV light beam to circumvent scattering media. In this experiment, the depolarization of light in TM as a function of incident OAM value is investigated for large particles ($d>\lambda$) and small ($d< \lambda$) where d is the particle diameter and λ is the light's wavelength. The SOP for large particles retains its polarization due to the small angles of scattering in the forward direction for photons observed in the backward and ninety-degree direction.

As shown in Figure 4 a linear polarized Gaussian beam from a Helium-Neon laser cavity (633nm, ~5mW) is expanded and collimated to a beam waist of ~5mm and converted into an OV baring light beam using a reflective, phase only, spatial light modulator (HOLOEYE) that displays a 'fork' diffraction grating. The OV light beam is selected in the first diffraction order of the far-field diffraction pattern by an aperture. The 'fork' grating is made via custom MATLAB software and directly related to the OAM of the generated OV light beam; by changing the 'fork' pattern we can dynamically and controllably change the light beam's OAM. The SOP of the OV light beam is controlled by its propagation through a quarter wave plate (QWP) and half wave plate HWP in series. In total, we can tailor a light beam with an arbitrary OAM and elliptical SOP. The SOP of the OV light beam is set to horizontal (*H*) or vertical (*V*) polarization, and is then focused by a lens (f=10cm) into a rectangular quartz cell of dimension 1cm x 10 cm x 10cm containing a mixture of distilled water and micron sized latex spheres (n=1.5) from which it scatters. The resulting right angle scattered light is collected with a pair of lenses and imaged onto a photodiode that measures the light's intensity using a digital oscilloscope. The intensity of the *H* and *V* components of the scattered light intensity is analyzed using a properly oriented linear polarizer before the photo-detector. The light's depolarization is denoted $i(j)$ being the incident(scattered) light SOP, respectively. The experiment consists of measuring the intensity of the *H* and *V* components of the scattered light for each input H or V SOP as a function of OAM value ℓ. This is done for varying scattering particle concentration and size. The particle sizes are chosen to be larger and smaller than the light's wavelength.

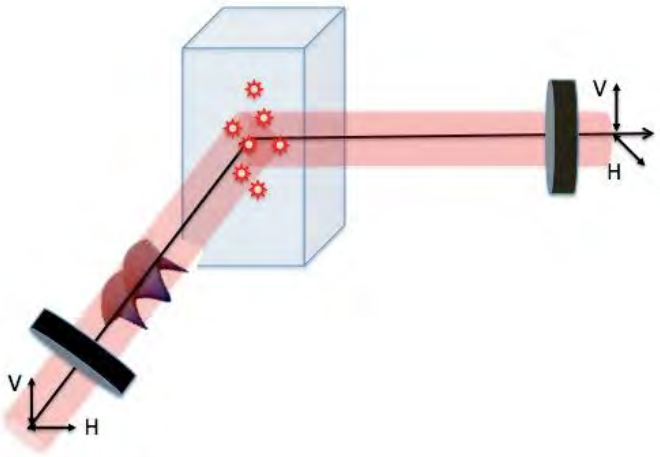

Figure 4. Experimental setup for OAM dependence on right angle depolarization. An OV light beam with a helical wave front is incident on a scattering media for incident H and V polarization. The scattered light is collected and analyzed at H and V polarization using a linear polarizer.

The experimentally measured intensity of the scattered light as a function of incident OAM value for scattering particles of varying size and concentration is plotted in the graphs of Figure 5. Examining the graphs of Figure 5 it can be seen that the intensity of the scattered light clearly depends on the incident OAM value ℓ for both large and small particles. The scattered light intensity decreases as ℓ increases. This may be due in part to the increasing azimuthal energy flow of the OV light beam as the OAM is increased. The spiraling energy flow may circumvent the scattering particles. The OAM seems to have an inverse proportionality indicating a 'saturation' of the OV ability to circumvent the TM. This may be associated with decoherence of the OV as it penetrates deeper into the medium. A theoretical investigation of the OAM dependent scattering and transmission measurements will be undertaken in the third year and out years.

It can be seen for particles larger than the light's wavelength the intensity of the co-polarized polarization intensity, H(H) and V(V), is nearly the same. Additionally, the intensity of the perpendicular polarized components is nearly zero. This indicates that the polarization of the scattered light is largely preserved even at a right angle. We refer to this as a polarization memory effect for linear polarization. Large particles, larger than the incident light's wavelength, scatter mostly in the forward direction. The preservation of the SOP of the light scattered at a right angle may be associated with a multiple scattering process that turns the light's direction of propagation.

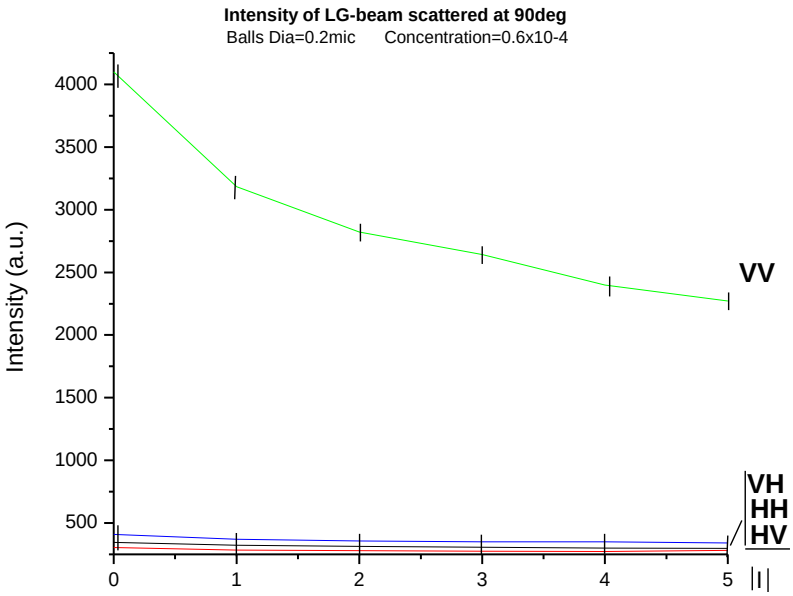

Figure 5(a)

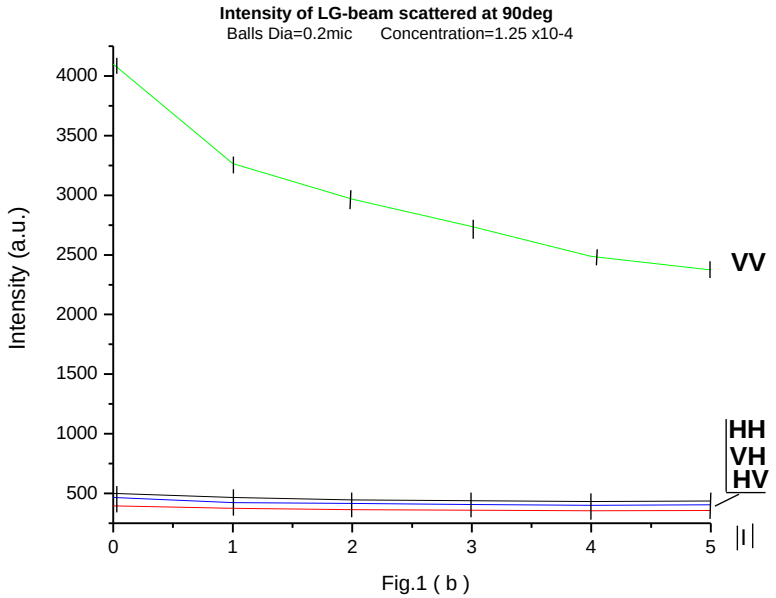

Figure 5(b)

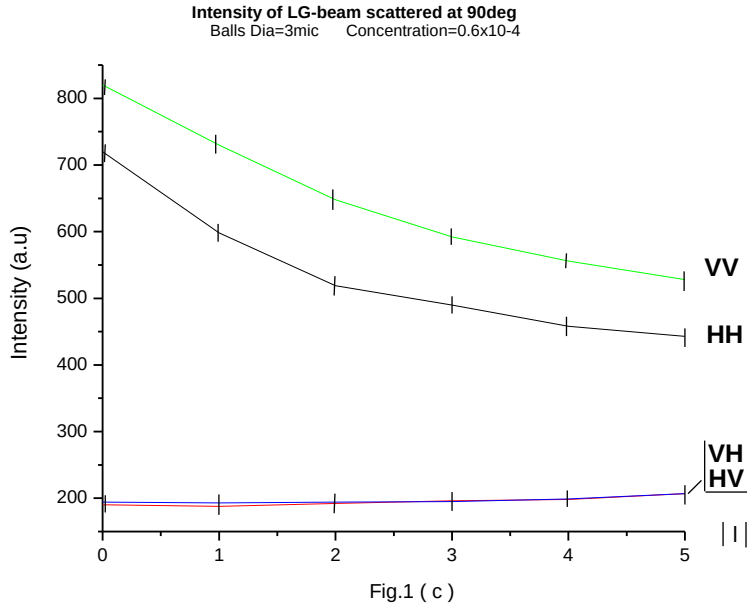

Figure 5(c)

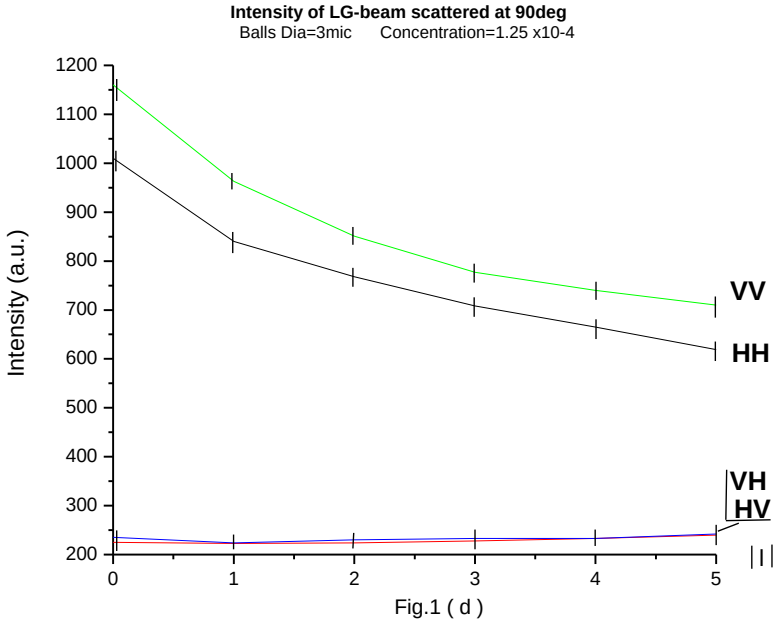

Figure 5(d)

Figure 5. Scattering intensity for input and output H and V SOP as a function of input OAM value particle sizes 0.2 microns at a concentration of (a) 0.6x10-4 and (b)1.25x10-4. Particle size 3.0 microns at a concentration of (c) 0.6x10-4 and (d) 1.25x10-4

3. OAM Dependence on Polarization Resolved Image Contrast

Seeing an object inside a TM can be improved by looking at the light corresponding to a specific SOP. It has been shown that the contrast of an image in TM is the highest when the image is illuminated with circular polarized light and then viewed at the orthogonal circular polarization or when illuminated with horizontal polarized light and viewed at parallel horizontal polarization. We experimentally investigate the dependence of OAM on this polarization resolved image contrast in TM in the backscattered direction.

As shown in Figure 6 a linear polarized Gaussian beam from a Helium-Neon laser cavity (633nm, ~5mW) is expanded and collimated to a beam waist of ~5mm and converted into an OV baring light beam using a reflective, phase only, spatial light modulator (HOLOEYE) that displays a 'fork' diffraction grating. The OV light beam is selected in the first diffraction order of the far-field diffraction pattern by an aperture. The 'fork' grating is made via custom MATLAB software and directly related to the OAM of the generated OV light beam; by changing the 'fork' pattern we can dynamically and controllably change the light beam's OAM. The SOP of the OV light beam is controlled by its propagation through a quarter wave plate (QWP) and half wave plate HWP in series. In total, we can tailor a light beam with an arbitrary OAM and elliptical SOP. The SOP of the OV light beam is set to horizontal (*H*) or right circular (*R*) polarization, and is then focused by a lens (f=10cm) into a rectangular quartz cell of dimension 10cm x 10 cm x 10cm containing a mixture of distilled water and micron sized latex spheres (n=1.5) from which it scatters. The OV light beam illuminates an Air Force target placed within the scattering media target as shown in Figure 6. The target is imaged onto a CCD camera.

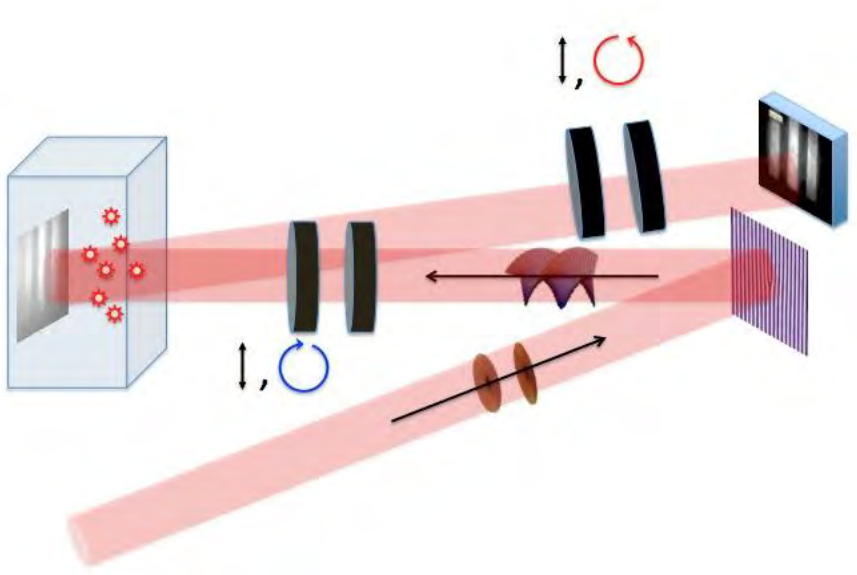

Figure 6. Experimental setup for OAM dependence on polarization resolved image contrast. A linear polarized pane wave Gaussian beam from a He-Ne laser is converted into an OV light beam with a helical wave front using a SLM displaying a fork diffraction grating. The SOP of the OV light beam is controlled using a half wave plate and quarter wave plate in series.

The intensity of the polarization of the backscattered image is selected using a LP and QWP in series to select out the H or R polarization of the scattered light. Intensity images fort H and R polarization of the target as recorded with the CCD camera as a function of OAM value ℓ for varying particle sizes and concentration are shown in three panels in Figure 7 for unpolarized, circular polarized, and linear polarized. The particle sizes are chosen to be larger and smaller than the light's wavelength.

3.1. Image enhancement using orbital angular momentum degradation

Figures 7 and 8 plots the backscattered image contrast for as a function of OAM value for scattering particles larger than the light's wavelength. It is clearly seen that when illuminating the target with circular polarized light and imaging the opposite circular polarization provides an enhanced image contrast over imaging the total 'unpolarized' intensity. This enhanced image contrast is even greater than when imaging with co-linear polarized light for H polarization. The physical mechanism for the enhanced image contrast is a circular polarization memory effect of light.

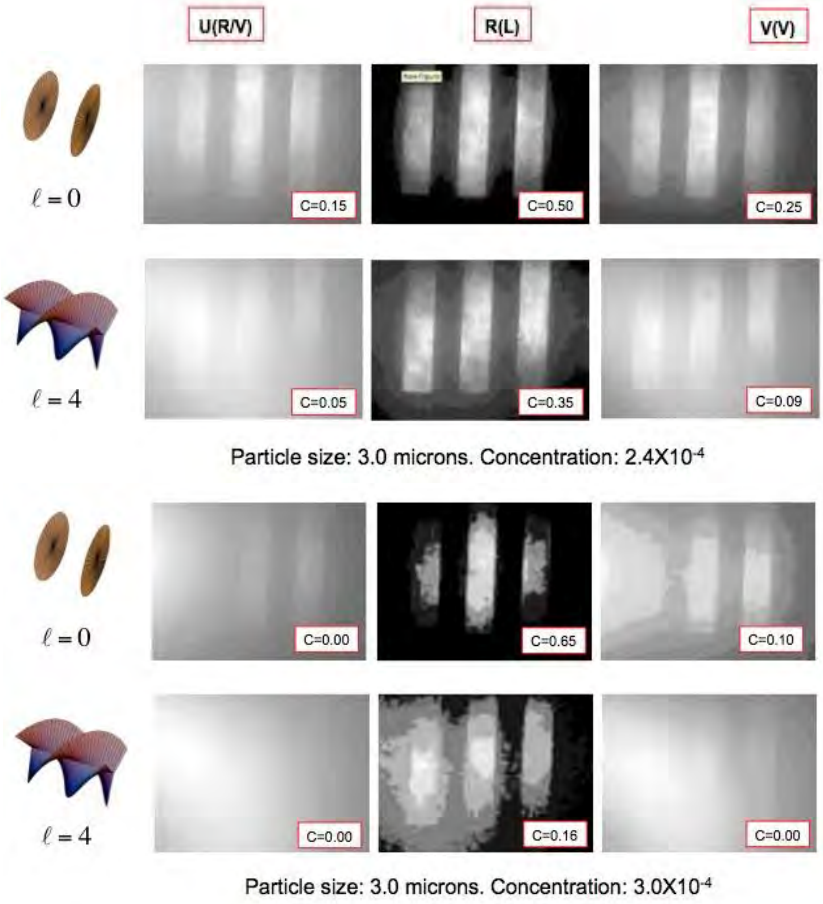

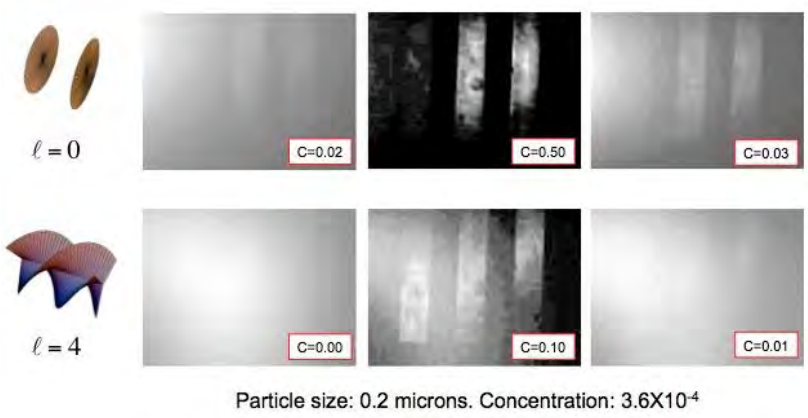

Figure 7. OAM dependence on polarization resolved image contrast

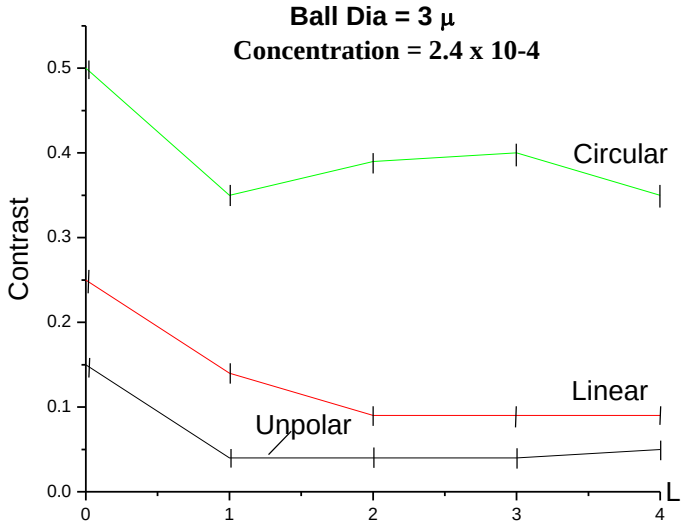

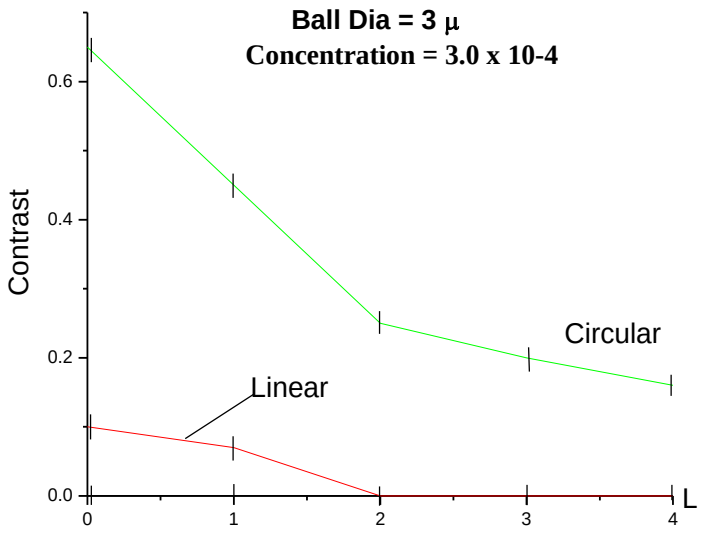

Figure 8. Contrast for circularly and linearly polarized light for large particles.

4. Tunable optical vortex

The experimental set-up for the optical spectral filter is as follows: multicolored supercontinuum light is generated using a PC fiber and made to be linearly polarized as described in the first scheme. The beam is then sent through a q-plate of q = 1 and the light coupled into a SMO fiber, with cut-off wavelength at 416 nm. An objective lens with numerical aperture of NA=0:4 is used to couple light through free space into SMO fiber with NA=0:12. The resulting beam is imaged onto a CCD camera. The experimental set-up is presented in Fig 9(b).Focusing the vortex light should create small spot size, and efficient coupling of non-vortex light into SMO fiber. For multicolored coherent vortex field at focus of numerical aperture lens, the spectrum along a closed loop enclosing the phase singularity undergoes rapid changes as the point of observation moves along the loop. Due to diffraction, there is a spatial redistribution of the spectral components such that when a certain spatial region is selected there will be a blue shift or red shift of the entire spectrum due to this redistribution. The spectral properties, i.e. wavelength channels, of the multicolored spectra within the bandwidth of the SMO fiber are preserved as the light propagates through the fiber.

As the external voltage applied to the q-plate is tuned from 2.50 V to 2.00 V in steps of 0.25 V, the q-plate is resonant" for particular wavelengths and detuned from other wavelengths. This breaks modal symmetry of a single vector vortex mode, and there is spatial redistribution of spectral components in multicolored mode, which changes the coupling efficiency of particular colors into the SMO fiber. Fig. 9(a) shows an example of the multicolored optical mode going into the SMO fiber at a particular voltage. As a result, the light coming out of the SMO fiber changes color from orange to yellow to green in incremental steps as presented in Fig. 9(b) to (d). The purity of colors in the spatially coherent optical intensity profile coming out of the SMO fiber is quantified in a bar chart containing an RGB (Red, Green, Blue) color analysis; and also presented in Fig. 9(b) to (d). This demonstrates the feasibility of the device as a tunable spectral filter using the SAM to OAM conversion of light by the q-plate. We note that only the TEM00

gaussian mode is coupled into the SMO fiber, and the higher order modes addressed by the q-plate are filtered out. The scheme can therefore serve as an optical switch to tune between different frequency channels in the HMWDM scheme described earlier.

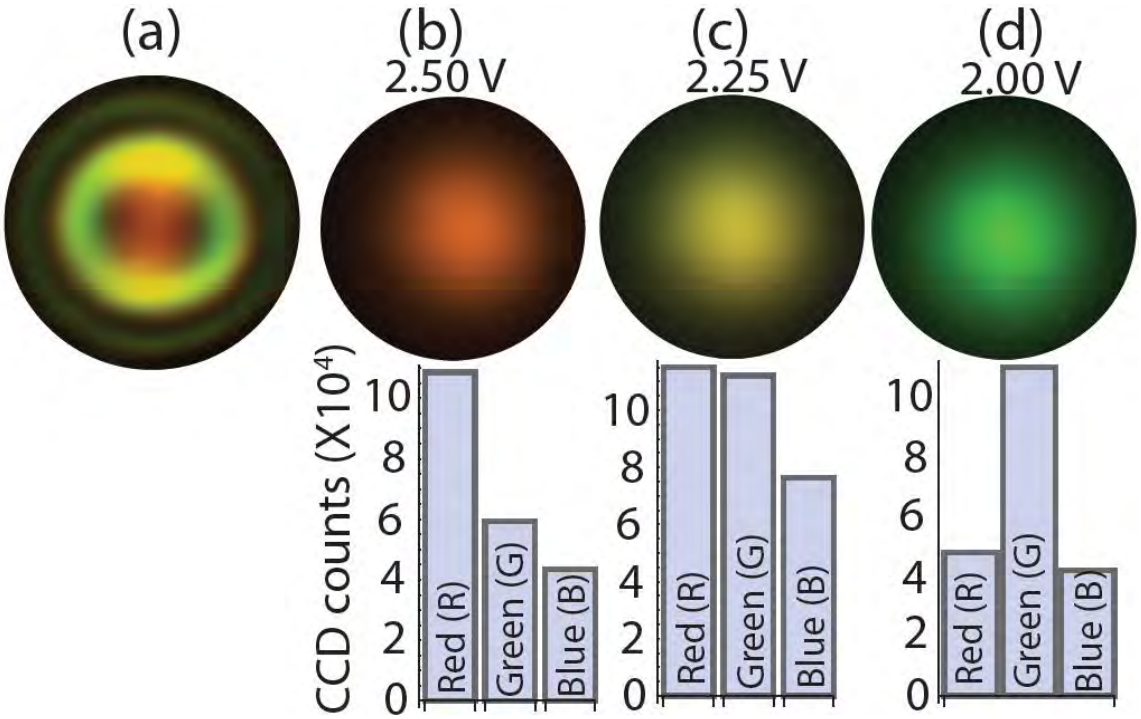

Figure 9. Experimental data demonstrating optical spectral filter. (a) Example of multicolored optical mode generated by q-plate and going into SMO fiber. As the voltage through the q-plate is tuned from 2.50 V to 2.00 V the colors emerging from the SMO fiber changes from orange to yellow to green as shown in (b), (c), (d). CCD counts represent the total counts for each RGB color on CCD screen, where counts in each pixel is normalized to a value between 0 and 1, and actual CCD counts range
from 0 to 255.

Optical vector vortex beams possessing OAM have been created using a multicolored supercontinuum laser light source and a tunable q-plate. Together with a single mode fiber, this effect can be used as a wavelength selective optical filter, or \optical switch" to move between different frequency channels in a communication network, especially in HMWDM scheme. The scheme is not limited to optical communications, but can be applied in the development of cost effective STED fluorescence microscopy systems with sub-diffraction resolution, such that tuning is achieved between different colors of the optical vortices by simply changing the electric field going through the q-plate.

There are several unfinished experiments to be addressed in this program. Several state of the art equipment has been acquired just before the end of this grant from other funding sources and was not used. In particular, Q-plates from Italy, vector beam sorter from UK, and two SLMs from Hamamatsu (ordered but not received yet). New graduate student Ms. Thienan Nguyen started training in this research area during the last academic year and past summer to work on generation of incoherent OV beams, and speckle spatial frequencies. Funds are needed to complete this program.

Publications

1. “Cylindrical vector beam generation from a multicore optical fiber,” Giovanni Milione, H. I. Sztul, D. A. Nolan, J. Kim, M. Etienne, J. McCarthy, J. Wang, and R. R. Alfano, Proc. SPIE Int. Soc. Opt. Eng. 7950, 79500K (2011)

2. “Geometric phase associated with transformations of cylindrical vector beams,” G. Milione, H. I. Sztul, and R. R. Alfano, Proc. SPIE Int. Soc. Opt. Eng. 7950, 79500S (2011)

3. “Hybrid vector beam generation,” G. Milione, S. Evans, and R. R. Alfano, Proc. SPIE Int. Soc. Opt. Eng. 7950, 79500Z (2011)

4. “Raman Optical Avtivity by Light with Spin and Orbital Angular Momentum,” G. Milione, J. Secor, S. Evans, G. Michel, and R. R. Alfano, Proc. SPIE Int. Soc. Opt. Eng. 7950, 79500H (2011)

5. "Cylindrical vector beam generation from a multi elliptical core optical fiber," G. Milione, H. I. Sztul, D. A. Nolan, J. Kim, M. Etienne, J. McCarthy, J. Wang, and R. R. Alfano, in *CLEO:2011 - Laser Applications to Photonic Applications*, OSA Technical Digest (CD) (Optical Society of America, 2011), paper CTuB2.

6. "Cylindrical Vector Beam Transformations and Hybrid Vector Beams," G. Milione, S. Evans, and R. Alfano; Frontiers in Optics, OSA Technical Digest (CD) (Optical Society of America, 2010), paper FWC4

7. "Geometric Phase and Poincare Sphere for Cylindrical Vector Beams," G. Milione, H. Sztul, and R. Alfano; Frontiers in Optics, OSA Technical Digest (CD) (Optical Society of America, 2010), paper JTuA04.

8. “Higher order Poincare Sphere, Stoke Parameters, and the Angular Momentum of Light,” G. Milione; Physical Review Letters 107, 053601 (2011)

9. “Higher-Order Pancharatnam-Berry phase and the Angular Momentum of Light,” Giovanni Milione, S. E. Evans, D. A. Nolan, and R. R. Alfano, Physical Review Letters 108 (19), 190401 (2012)

10. “The Geometric Phase and Singular Light Beams,” Giovanni Milione, S. E. Evans, D. A. Nolan, R. R. Alfano, Conference on Lasers and Electro-Optics (CLEO), paper JTh3K.6, (2012)

11. “A Higher Order Poincare Sphere Representation,” Giovanni Milione and R. R. Alfano, Proc. SPIE Int. Soc. Opt. Eng. 8274, 827407 (2012)

12. “Vector Beam Representation on a Higher Order Poincare Sphere …” Giovanni Milione and R. R. Alfano, Frontiers in Optics, OSA Technical Digest paper FThQ4, (2011)

13. Milione, Giovanni, S. Evans, D. A. Nolan, and R. R. Alfano. "Higher order Pancharatnam-Berry phase and the angular momentum of light." Physical Review Letters 108, 190401 (2012)

14. Milione, Giovanni, S. Evans, Dan A. Nolan, and Robert R. Alfano. "The geometric phase and singular light beams." In *Lasers and Electro-Optics (CLEO), 2012 Conference on*, pp. 1-2. IEEE, (2012)

15. Milione, Giovanni, and Robert R. Alfano. "A higher order Poincare sphere representation." *Proceedings of SPIE*. Vol. 8274 (2012)

16. Milione, Giovanni and Robert R. Alfano, "Vector Beam Representation on a Higher Order Poincare Sphere and Higher Order Stokes Parameter Measurement Through Optical Angular Momentum Decomposition," Frontiers in Optics, OSA Technical Digest (CD) (Optical Society of America, 2011), paper FThQ4

17. Pavel Shumyatsky, Giovanni Milione, and Robert R Alfano, Optical Memory Effect from Polarized Laguerre-Gaussian Light Beam in Light-Scattering Turbid Media, Optics Communications, 321, 116-123 (2014).

Oral/Poster Presentations

1. "Cylindrical Vector Beam Transformations and Hybrid Vector Beams," G. Milione, S. Evans, and R. Alfano; OSA Frontiers in Optics Conference Rochester, NY October 2010

2. "Geometric Phase and Poincare Sphere for Cylindrical Vector Beams," G. Milione, H. Sztul, and R. Alfano; OSA Frontiers in Optics Conference Rochester, NY October 2010

3. "Singular Optics: Theory and Applications," G. Milione, H. I. Sztul, and R. R. Alfano, Poster presentation Herman Z. Cummins Symposium, the City College of New York, New York, NY October 2010

4. "Cylindrical vector beam generation from a multicore optical fiber," G. Milione, H. I. Sztul, D. A. Nolan, and R. R. Aflano; SPIE Photonics West, Complex Light and Optical Forces V San Francisco, CA January 2011

5. "Geometric phase associated with transformations of cylindrical vector beams," G. Milione, H. I. Sztul, and R. R. Aflano; SPIE Photonics West, Complex Light and Optical Forces V San Francisco, CA January 2011

6. "Hybrid vector beam generation," G. Milione and R. R. Alfano; SPIE Photonics West, Complex Light and Optical Forces V San Francisco, CA January 2011

7. "Raman Optical Avtivity by Light with Spin and Orbital Angular Momentum," G. Milione, J. Secor, S. Evans, G. Michel, and R. R. Alfano, SPIE Photonics West, Complex Light and Optical Forces V San Francisco, CA January 2011

8. "Cylindrical vector beam generation from a multi elliptical core optical fiber," G. Milione, H. I. Sztul, D. A. Nolan, J. Kim, M. Etienne, J. McCarthy, J. Wang, and R. R. Alfano, OSA CLEO Conference Baltimore, MD May 2011

9. “Complex and Structured Light in Photonics: Singular Optical Beams,” G. Milione, Einsteins in the City Conference, the City College of New York, New York, NY April 2011

10. Singular Optics: Optical Phase and Polarization Gradients,” G. Milione, New York University, Physics Department, Center for Soft Matter Research April 2011

11. “Optical Spin and Orbital Angular Momentum and a Higher Order Poincare Sphere: Implications and Applications,” Giovanni Milione; Pan-American Advanced Science Institute on Frontiers in Imaging Science, Bogota Colombia June 2011

12. “Higher Order Poincare Sphere, Stokes Parameters, and the Angular Momentum of Light,” Giovanni Milione; Singular Optics Workshop and Applications to Modern Physics, Abdus Salam International Center for Theoretical Physics, Trieste Italy June 2011

13. “Introduction to the Orbital Angular Momentum of Light,” G. Milione, Invited Talk Laser Teaching Center Stony Brook University July 2011

14. “The Geometric Phase and Singular Light Beams,” Giovanni Milione, S. E. Evans, D. A. Nolan, R. R. Alfano, Conference on Lasers and Electro-Optics (CLEO), paper JTh3K.6, (2012)

15. “A Higher Order Poincare Sphere Representation,” Giovanni Milione and R. R. Alfano, Proc. SPIE Int. Soc. Opt. Eng. 8274, 827407 (2012)

16. “Vector Beam Representation on a Higher Order Poincare Sphere …” Giovanni Milione and R. R. Alfano, Frontiers in Optics, OSA Technical Digest paper FThQ4, (2011)

17. Milione, Giovanni, S. Evans, Dan A. Nolan, and Robert R. Alfano. "The geometric phase and singular light beams." In *Lasers and Electro-Optics (CLEO), 2012 Conference on*, pp. 1-2. IEEE, (2012)

18. Milione, Giovanni, and Robert R. Alfano. "A higher order Poincare sphere representation." *Proceedings of SPIE*. Vol. 8274 (2012)

19. Milione, Giovanni and Robert R. Alfano, “Vector Beam Representation on a Higher Order Poincare Sphere and Higher Order Stokes Parameter Measurement Through Optical Angular Momentum Decomposition,” Frontiers in Optics, OSA Technical Digest (CD) (Optical Society of America, 2012), paper FThQ4

20. Invited Talk: Giovanni Milione, International Conference on Orbital Angular Momentum, Glasgow, UK

21. Invited Talk: Giovanni Milione SPIE Complex Light and Optical Forces Conference VII, San Francisco, CA

22. Invited Talk: Giovanni Milione: Singular Optics Conference and Application to Modern Physics, Trieste Italy

High School/Undergraduate Oral/Poster Presentations

1. "Optical Vortex Beam generation using a spatial light modulator," Fuad Zaher, Midwood High School Midwood, NY, *Semifinalist* New York City Science and Engineering Fair (NYCSEF) Competition 2011

2. "Optical Vortex Beam generation using a spatial light modulator," Fuad Zaher, Midwood High School Midwood, NY, *Semifinalist* St Josephs College Science competition 2011

3. "Optical Vortex Beam generation using a spatial light modulator," Fuad Zaher, Midwood High School Midwood, NY, Intel Science Competition 2011

4. "Cylindrical vector beam generation from multi-elliptical core fiber," Jonathan Kim, Flushing high school NYC, *Semifinalist* NYCSEF Competition 2011

5. "Optical Vortex Party," High School/Undergraduate Optics Research Symposium at Stony Brook University, Fuad Zaher, Jonathan Kim, and Stefan Evans July 2011

Awards

1. National Science Foundation Graduate Research Fellowship, Giovanni Milione 2011

2. SPIE International Society of Optics and Photonics Scholarship, Giovanni Milione 2011

3. Finalist, Emil Wolf Outstanding Student Paper Competition, Giovanni Milione (2011)

4. Robert R. Alfano, American Physical Society, Arthur L. Schawlow Prize in Laser Science (October, 2013)

5. Robert R. Alfano, City College of New York, President's Award For Excellence (2013)

6. Robert R. Alfano, Association of Italian-American Educators, Lifetime Achievement Award (2012).

7. Giovanni Milione, Optical Society of America, Finalist Emil Wolf Outstanding Student Paper Competition.